ISSN 1807-1929
Revista Brasileira de Engenharia Agrícola e Ambiental
Brazilian Journal of Agricultural and Environmental Engineering
v.28, n.6, e281097, 2024
Campina Grande, PB – http://www.agriambi.com.br – http://www.scielo.br/rbeaa

DOI: http://dx.doi.org/10.1590/1807-1929/agriambi.v28n6e281097 ORIGINAL ARTICLE

Design and optimization of energy consumption in hydroponic greenhouse[1]

Projeto e otimização do consumo de energia em estufa hidropônica

Islem B. Hassine[2*], Dhafer Mezghani[2], Anouar Belkadi[2], Nizar Sghaier[3] & Abdelkader Mami[2]

[1] Research developed at University of Tunis El Manar, El Manar, Tunıs, Tunısıa
[2] University of Tunis El Manar/Faculty of Sciences of Tunis, El Manar, Tunıs, Tunısıa
[3] University of Tunis El Manar/Faculty of sciences of Tunis/Laboratory for Research on Microwave Electronics, El Manar, Tunıs, Tunısıa

HIGHLIGHTS:

Optimizing lighting systems leads to substantial energy savings and improved production in hydroponic greenhouses.
The interplay between lighting, heating, and cooling enables more efficient energy consumption and enhanced crop yield.
Hydroponic greenhouse design and choice of cover material significantly influence energy balance and environmental impact.

ABSTRACT: Achieving the optimal energy balance in hydroponic greenhouses is a critical challenge in modern agriculture. This involves managing energy resources to create an environment conducive to robust crop growth. Researchers are exploring advanced thermal models and innovative technologies to enhance energy efficiency and establish a harmonious equilibrium in these controlled environments. Various studies have addressed the optimization of energy consumption in hydroponic greenhouses, with a focus on the greenhouse covering materials and real-time energy monitoring. This study aims to enhance the conventional model by optimizing the form and cover material of the greenhouse and considering new heat gain and loss parameters, including the direct and indirect lighting effect. This study demonstrates that the emitted light and energy consumption of the lighting system directly influence the energy balance. This innovative approach refines the understanding of the interplay between lighting systems and energy consumption, leading to more efficient and sustainable hydroponic greenhouse practices. Collectively, the contributions of esteemed researchers have significantly enriched the understanding of energy consumption dynamics in hydroponic greenhouse environments, setting new standards for energy efficiency, sustainability, and productivity in hydroponic agriculture.

Key words: cooling, energy project, heating, lighting

RESUMO: Conseguir um equilíbrio energético ótimo em estufas hidropônicas é um desafio crítico na agricultura moderna. Isto implica a gestão dos recursos energéticos para criar um ambiente propício a um crescimento robusto das culturas. Os pesquisadores estão a explorar modelos térmicos avançados e tecnologias inovadoras para melhorar a eficiência energética e estabelecer um equilíbrio harmonioso nestes ambientes controlados. Vários estudos abordaram a otimização do consumo de energia em estufas hidropônicas, com destaque para os materiais de cobertura das estufas e a monitorização da energia em tempo real. Este estudo visa melhorar o modelo convencional, otimizando a forma e o material de cobertura da estufa e considerando novos parâmetros de ganho e perda de calor, incluindo o efeito da iluminação direta e indireta. Este estudo demonstra que a luz emitida e o consumo de energia do sistema de iluminação influenciam diretamente o balanço energético. Esta abordagem inovadora melhora a compreensão da interação entre os sistemas de iluminação e o consumo de energia, conduzindo a práticas de estufa hidropônica mais eficientes e sustentáveis. Coletivamente, as contribuições de pesquisadores conceituados enriqueceram significativamente a compreensão da dinâmica do consumo de energia em ambientes de estufa hidropônica, estabelecendo novos padrões de eficiência energética, sustentabilidade e produtividade na agricultura hidropônica.

Palavras-chave: resfriamento, projeto energético, aquecimento, iluminação

• Ref. 281097 – Received 04 Dec, 2023
* Corresponding author - E-mail: islem.benhassine92@gmail.com
• Accepted 08 Feb, 2024 • Published 25 Mar, 2024
Editors: Toshik Iarley da Silva & Carlos Alberto Vieira de Azevedo

Introduction

To achieve an optimal energy balance in contemporary agricultural practices, especially within hydroponic greenhouses, the main challenge involves meticulous management of energy resources to establish an environment conducive to robust crop growth.

Researchers have endeavoured to optimize energy consumption in hydroponic greenhouses through various means. Aryai et al. (2022) focus on developing the greenhouse energy balance while recognizing potential challenges associated with implementing this approach in resource-constrained settings. Gillani et al. (2022) have set new benchmarks for sustainable and efficient food production, especially in the selection of greenhouse covering materials. Despite significant progress in dynamic greenhouse models, Bouadila et al. (2023) acknowledge complexities associated with their implementation, addressing the critical aspect of greenhouse covering materials. Cannarsa et al. (2023) emphasize the importance of reducing energy consumption while recognizing the potential technical challenges related to photosynthesis, particularly in the use of CO_2 generators and the direct aspect of artificial lighting. Zaborowska et al. (2021) make a remarkable contribution to energy balance and reduction by modeling plant evapotranspiration. Delgado et al. (2020) present energy efficiency gains through the use of photo-selective films, prompting further exploration of scalability and cost-effectiveness. Providing valuable insights into innovative lighting solutions for energy-efficient greenhouses, Ezzaeri et al. (2018) call for further research into specific roofing materials.

In this study, the objective is to improve the traditional greenhouse model by optimising its shape and covering material. Additionally, new factors are considered such as the direct and indirect effects of lighting. This innovative approach deepens the understanding of the impact of lighting systems on energy usage and ultimately promotes more efficient and environmentally friendly hydroponic greenhouse methods. The study aims to contribute to the existing body of knowledge by addressing research gaps and offering practical insights for the sustainable advancement of hydroponic greenhouse technology.

Material and Methods

In this study, five different types of greenhouses were examined (Figure 1). These included even span, uneven span, elliptic, Quonset, and vinery designs. While each greenhouse varied in shape and structure, all were constructed to have the same volume of 4,220 m^3 and base area of 1,360 m^2. By analyzing different types of greenhouses, a better understanding of how each design affects the energy efficiency and overall performance of the system can be gained.

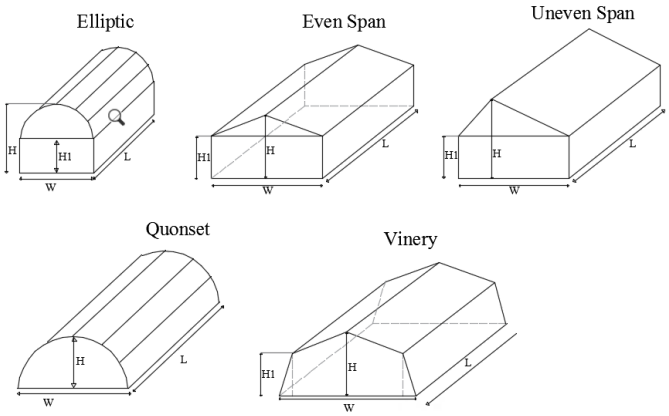

W - Width of the greenhouse (m); H1- Eaves height of the greenhouse (m); H - Ridge height of the greenhouse (m); L - Length of the greenhouse (m)

Figure 1. Greenhouse form analysis

The study encompassed an analysis of six different hydroponic greenhouse-covering materials, each one with distinct properties and characteristics. Table 1 provides a comprehensive overview of these materials, outlining their unique features and labelling them as M1 through M6.

When establishing the energy balance of a hydroponic greenhouse, a range of climatic parameters must be taken into account to effectively manage the conditions inside the greenhouse. Heat transfer and mass exchange between the indoor and outdoor environment are key factors that determine the energy balance of the greenhouse. The general equation (Eq. 1) for the heat balance of a hydroponic greenhouse is as follows (Al-Karaki et al., 2009; Akram et al., 2020).

$$Q_{syst} = (Q_L - Q_G) = (Q_{cd-cv} + Q_{water} + Q_{inf}) - (Q_{sr}) \quad (1)$$

where:

Q_{syst} - total required heating and cooling power (W);
Q_L - total heat losses from the greenhouse (W);
Q_G - total heat gain inside the greenhouse (W);
Q_{cd-cv} - conduction and convection heat transfer (W);
Q_{water} - water heat transfer (W);
Q_{inf} - heat loss from infiltration (W); and,
Q_{sr} - heat gain from solar radiation (W).

In the context of an energy balance, a positive Q_{syst} indicates that the hydroponic greenhouse needs to be heated because the

Table 1. Characteristics of the materials used for covering (Luna-Fletes et al., 2021)

Characteristics	Glass	Low emission glass	Polyethylene film	Polycarbonate	Polyvinyl chloride	Ethylene-vinyl acetate
Abbreviation	M1	M2	M3	M4	M5	M6
Lc	0.003	0.0032	0.000152	0.01	0.0001	0.00015
Solar transmission	0.905	0.78	0.87	0.9	0.91	0.89
Long-wave transmission	3	<3	50	<3	<3	<3
Kc	0.76	0.76	0.33	0.17	0.13	0.38
ACH	1.1	1.1	0.85	1.1	0.8	0.82

Lc - Covering material thickness (m); Kc - Thermal conductivity (W m^{-1} K^{-1}); ACH - Number of air changes per hour (m^3 s^{-1}); M1 - Glass covering; M2 - Low emissivity glass covering; M3 - Polyethylene film covering; M4 - Polycarbonate covering; M5 - Polyvinyl chloride covering; M6 - Ethylene-vinyl acetate copolymer EVA covering

heat loss is greater than the heat gain. Conversely, a negative Q_{syst} suggests that the greenhouse needs to be cooled because the heat gain exceeds the heat loss, and this is necessary to maintain the ideal interior temperature for crops, light, and humidity. Several climatic factors such as the amount of radiation, wind speed, external temperature, and external humidity levels affect the heat loss of the greenhouse. In this study, the geometric design of the greenhouse has been described and the position of the greenhouse has been defined, which directly affects its energy balance. Table 1 presents the characteristics of the different roofing materials chosen for the study.

The approach is primarily based on the outcomes of the previous intermediate models, which have furnished valuable insights into the factors that have a significant impact on the energy balance. These theoretical findings have laid the groundwork for the current study (Belkadi et al., 2019).

In the conventional methodology, the net heat gain Q_G is calculated using the following Eq. 2.

$$Q_G = A_f \times \tau \times I_{sr} \quad (2)$$

where:

A_f - greenhouse floor area (m^2);

τ - transmissivity of the greenhouse cover; and,

I_{sr} - solar radiation on the horizontal surface (W m^{-2}).

The calculation of heat loss in a hydroponic greenhouse is based on two fundamental values: conduction-convection heat transfer $Q_{cd\text{-}cv}$ and infiltration heat transfer Q_{inf}. These values are typically used to accurately determine the level of heat loss.

The conductive-convective heat transfer can be calculated using the following Eq. 3.

$$Q_{cd-cv} = U \times A_{GH} \times H \times \left(T_{in} - T_{ex}\right) \quad (3)$$

where:

U - static overall heat transfer coefficient (W m^{-2} K^{-1});

A_{GH} - hydroponic greenhouse area (m^2);

H - height of the hydroponic greenhouse (m);

T_{in} - inner air temperature (°C); and,

T_{ex} - average outdoor temperature (°C).

The overall heat transfer coefficient in a closed hydroponic greenhouse is represented by U. This value remains constant, allowing the heat loss caused by infiltration Q_{inf} to be expressed as follows (Eq. 4).

$$Q_{inf} = A_{CH} \times \rho_a \times C_a \times V_G \times \left(T_{in} - T_{ex}\right) \quad (4)$$

where:

A_{CH} - number of air changes per hour (m^3 s^{-1});

ρ_a - density of internal air (kg m^{-3});

C_a - specific heat of air (J kg^{-1} K^{-1}); and,

V_G - volume of the hydroponic greenhouse (m^3).

An analysis of the heat transfer of the nutrient solution flowing through the main pipe of the hydroponic system should be conducted to establish the basis for designing a limited cooling system for the crop's root zone and to maintain the reservoir temperature in a controlled greenhouse (Belkadi et al., 2021). The rate of heat transfer through a pipe can be determined by using Eq. 5.

$$Q_{water} = U_{water} \times A \times \Delta T \quad (5)$$

where:

U_{water} - dynamic overall heat transfer coefficient of water (W m^{-2});

A - cross-sectional area of the object perpendicular to the heat flow (m^2); and,

ΔT- overall temperature between water and pipe surface (°C).

U_{water} can be expressed using Eq. 6.

$$U_{water} = \frac{2\pi \times K_p \times L_1}{\frac{A_2}{h \times A_1} + A_2 \times \ln\frac{D_2}{D_1}} \quad (6)$$

where:

K_p - thermal conductivity of pipe (W m^{-1} K^{-1});

A_1 - inner area of pipe (m^2);

A_2 - outer area of pipe (m^2);

D_2 - outer diameter of pipe (m);

D_1 - inner diameter of pipe (m);

L_1 - length of pipe (m); and,

h - convection coefficient between pipe wall and water (W m^{-2} K^{-1}).

The Reynolds number can be found using the following Eqs. 7, 8 and 9.

$$R_e = p \times V \times \frac{D_h}{u} \quad (7)$$

where:

R_e - Reynolds number;

P - density of the fluid (kg m^{-3});

D_h - hydraulic diameter (m);

u - dynamic viscosity of the fluid (kg m^{-1} s^{-1}); and,

V - fluid flow velocity (m s^{-1}).

$$D_h = D_2 - D_1 \quad (8)$$

$$h = K_a \times Nu \times V \times \frac{D_h}{u} \quad (9)$$

where:

K_a - thermal conductivity of water (W m^{-1} K^{-1}); and,

Nu - Nusselt number.

The study focuses on an even-span hydroponic greenhouse situated in Tunisia, with a total area of 1360 m^2. The greenhouse is located at a latitude of 36.84° and longitude of 10.14° and is covered with a glass film whose characteristics are provided above. To

simulate the heating and cooling requirements of the hydroponic greenhouse, meteorological data was collected and used. The temperature of the cultivated plants is maintained at 20.5 °C (Figure 2). From Figure 2, it is evident that the heating requirement is greatest in January when the average temperature is 12 °C. However, in April and November, despite having the same average temperature value, the heating need is higher in November. This suggests that the heating demand is not solely dependent on the number of sunshine hours and low temperatures.

Figure 3 represents a simulated model created using Matlab software.

The various types of hydroponic greenhouses, each covered with different films, have a substantial impact on the amount of heat loss or gain. After applying the heat transfer equations shown above, the resulting energy demand was calculated as follows (Table 2).

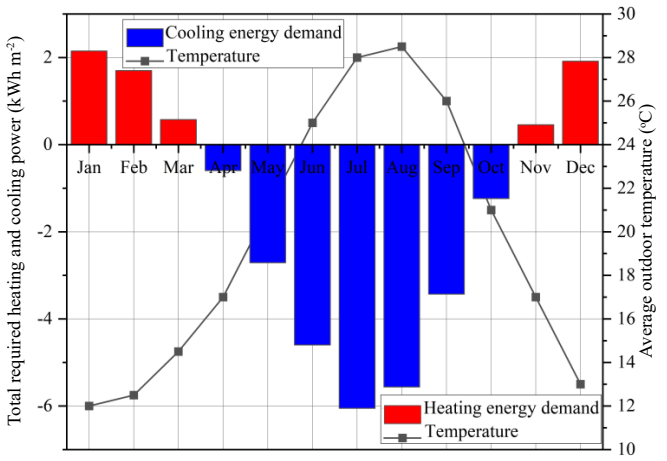

Figure 2. The energy requirements for heating and cooling using conventional methods

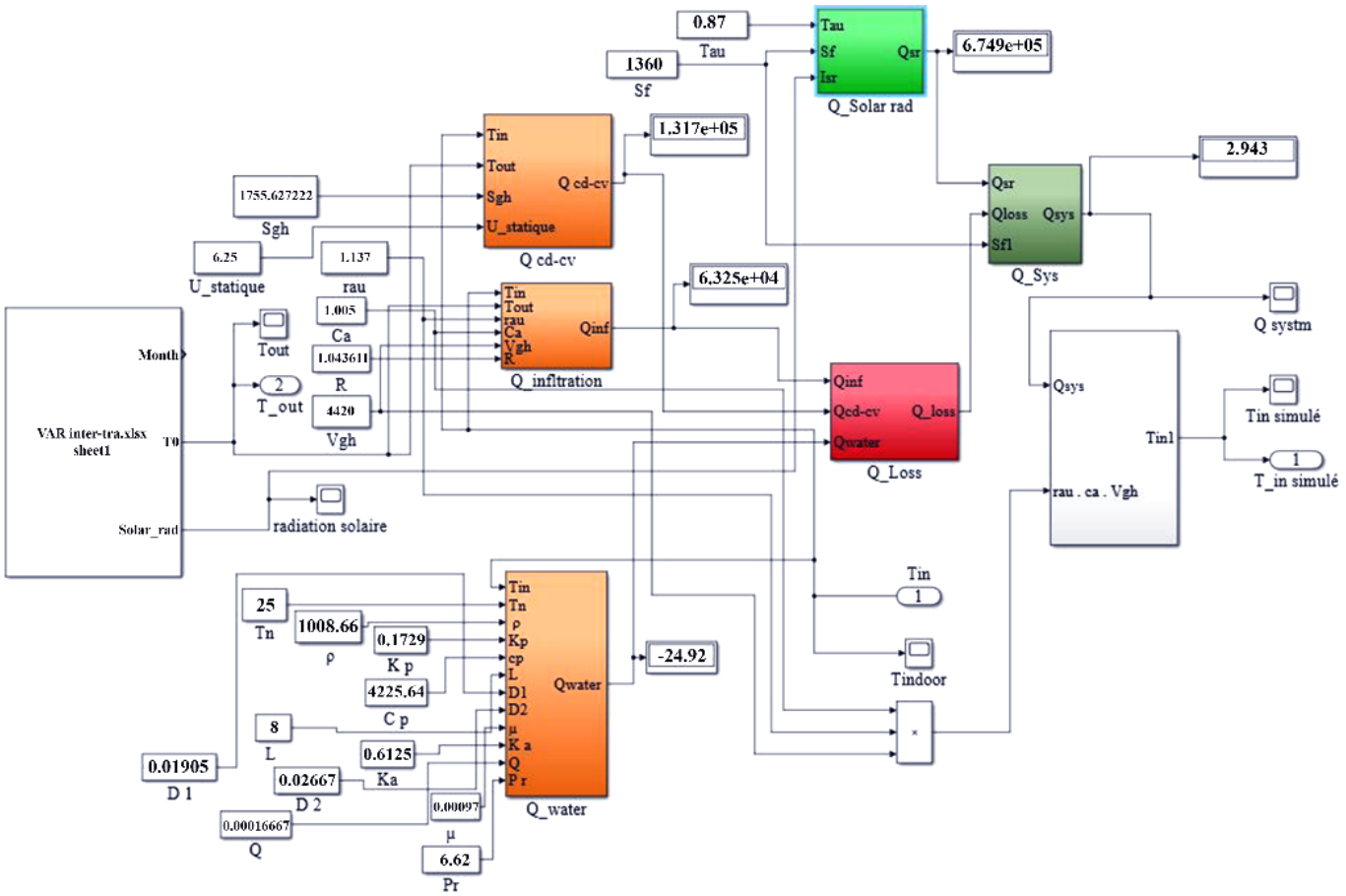

U_statique - Static overall heat transfer coefficient (W m^{-2} K^{-1}); SGH - Hydroponic greenhouse area (m^2); T_{in} - Inner air temperature (°C); T_{out} - Average outdoor temperature (°C); R - Number of air changes per hour (m^3 s^{-1}); Rau - Density of internal air (kg m^{-3}); C_a - Specific heat of air (J kg^{-1} K^{-1}); V_{gh} - Volume of the hydroponic greenhouse (m^3); K_p - Thermal conductivity of pipe (W m^{-1} K^{-1}); A_1 - Inner area of pipe (m^2); A_2 - Outer area of pipe (m^2); D_2 - Outer diameter of pipe (m); D_1 - Inner diameter of pipe (m); L - Length of pipe (m); p - Density of the fluid (kg m^{-3}); u - Dynamic viscosity of the fluid (kg m^{-1} s^{-1}); Pr - Prandtl coefficient; Ka - Thermal conductivity of water (W m^{-1} K^{-1}); Cp - Specific heat (J kg^{-1} K^{-1}); T_n - Temperature of solution (°C); Q - Water flow (m^3 s^{-1}); A_f - Greenhouse floor area (m^2); Tau - Transmissivity of the greenhouse cover; I_{sr} - Solar radiation on the horizontal surface (W m^{-2}); Sf - Floor surface (m^2)

Figure 3. Block simulink of the traditional model

Table 2. Application of the average daily heating and cooling demand using the traditional model in Tunisia

		Types of hydroponic greenhouses				
		Even span	Uneven span	Elliptic	Quonset	Vinery
Average cooling+heating (kWh m^{-2})	M1	-2.098168517	-2.093713817	-2.10401170	-2.128489545	2.12252377
	M2	1.621090774	-1.619175202	-1.62360341	-1.634129162	1.63156381
	M3	2.057222062	-2.052800262	-2.06302209	-2.087319158	2.08139744
	M4	2.354075688	-2.351581056	-2.35734787	-2.371055463	2.36771463
	M5	-2.278604989	-2.274611105	-2.28384372	-2.305789462	2.30044082
	M6	-2.074579465	-2.069729748	-2.08094079	-2.107589183	-2.1010944

M1 - Glass covering; M2 - Low emissivity glass covering; M3 - Polyethylene film covering; M4 - Polycarbonate covering; M5 - Polyvinyl chloride covering; M6 - Ethylene-vinyl acetate copolymer EVA covering

The design of a greenhouse, along with the covering material used, can significantly affect its energy consumption. By applying the heat transfer equations mentioned earlier and analyzing the results presented in Table 2, the uneven span shape with M2 covering material was found to be the most suitable, while the Quonset shape with M4 covering material was the least ideal.

This investigation into various energy balance calculation models indicates that the traditional model is inadequate since it fails to consider crucial parameters such as $U_{dynamic}$, Q_{lw}, Q_f, Q_p, Q_{evap}, Q_{co2}, and Q_{li}, which are essential in determining the state of a hydroponic greenhouse.

The value of $U_{dynamic}$, which represents the overall heat transfer coefficient, is affected by various factors, including the type of envelope used in the hydroponic greenhouse, the internal and external temperature, and the external and ambient wind speed. Depending on these factors, the value of $U_{dynamic}$ will vary, indicating the degree of heat transfer occurring between the greenhouse and its surroundings (Kumar et al., 2017).

Long-wave radiation exchange through the cover film $Q_{lw,}$ is a significant factor in heat loss within hydroponic greenhouses. Thermal radiation generated by the elements inside the greenhouse is reflected back into the greenhouse, emitted to the outside, or removed by the cover film, resulting in heat loss.

Soil conduction and perimeter heat transfer are the primary causes of heat loss in the soil of hydroponic greenhouses Q_p. It is essential to consider the impact of this heat loss in energy balance calculations to ensure the accuracy and consistency of the results. Ignoring these factors can lead to significant errors in the calculation and an incorrect estimation of the energy demand of the greenhouse.

Q_{evap} evaporation from the soil and transpiration of plants in hydroponic greenhouses result in a significant amount of heat loss. In this study, the energy balance calculation includes this component to accurately estimate the total energy demand of the greenhouse.

The instrumentation used to produce carbon dioxide in greenhouses can affect the heat gain in hydroponic greenhouses. When carbon dioxide is produced by burning fuel in the greenhouse, an excessive amount of heat Q_{co2} can be added to the environment.

Lighting in greenhouses can contribute a significant amount of heat to the environment. This quantity, referred to as Q_{li}, is a crucial element in accurately calculating the energy balance of a greenhouse. Prior studies neglected to account for the effect of heat released by the lamps, but it is an essential factor that must be considered to improve the accuracy of the energy balance calculation (Pawlowski et al., 2016; Belkadi et al., 2020).

The IBGH model is designed for the production of lettuce and the breeding of fish in a symbiotic system within a hydroponic greenhouse, taking into account the specific geographical and climatic parameters of Tunisia. The model improves upon conventional models by accounting for several previously unnoticed factors, including Q_{lw}, Q_f, Q_p, Q_{evap}, Q_{co2}, and Q_{li}, which considers the heat gains from artificial lighting. In addition, the total heat loss constant U is recalculated as a dynamic parameter in this model. Cooling, heating, and lighting are critical components to consider when calculating the energy balance of the hydroponic greenhouse and are strongly related to the shape of the greenhouse and its cover.

This model involves two main components. First, new parameters, such as Q_{lw}, Q_f, Q_p, Q_{evap}, and Q_{co2} have been added to more accurately calculate the energy balance. Second, the lighting heat gain parameter will be included, Q_{li}, which has been neglected in previous research. This highlights the importance of accounting for lighting when striving to maintain a highly energy-efficient environment.

To develop the model, the program depicted in Figure 4 was designed.

According to the developed IBGH model, the global heat transfer coefficient U will be dynamic in the calculation of heat loss by conduction and convection for transparent surfaces. It can be given as follows (Eq. 10).

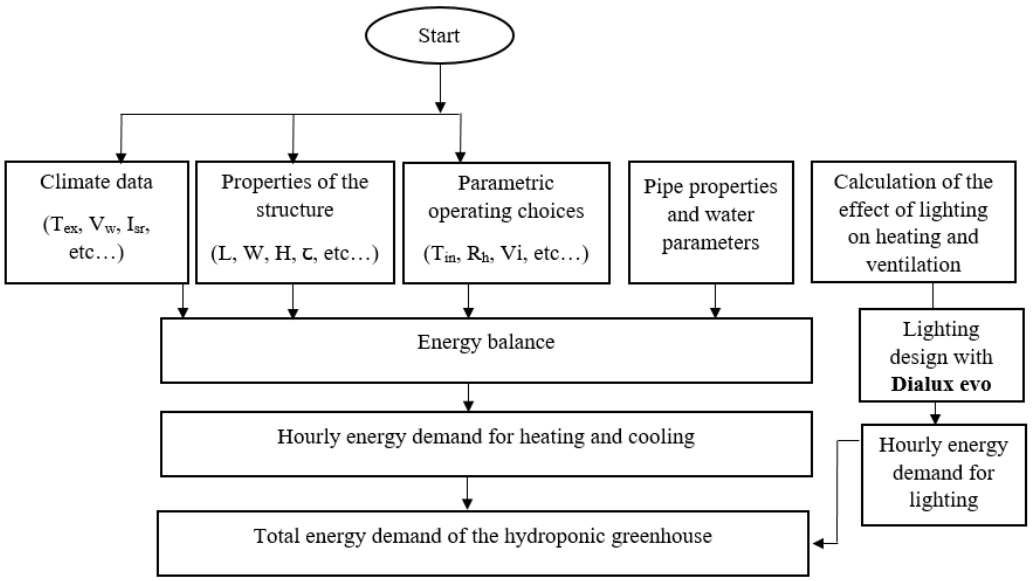

V_w - Wind velocity (m s^{-1}); W - Width of the greenhouse (m); V_i - Indoor air speed (m s^{-1}); I_{sr} - Solar radiation on the horizontal surface (W m^{-2}); T_{ex} - Average outdoor temperature (°C); L - Length of the greenhouse (m); H - Height of the greenhouse (m); τ - Transmissivity of the greenhouse cover; T_{in} - Inner air temperature (°C); R_h - Relative air humidity (%)

Figure 4. Examining the IBGH model without considering lighting

$$U_{dynamic} = \left(h_0^{-1} + L_c \times K_c + h_i\right)^{-1} \quad (10)$$

where:
$U_{dynamic}$ - dynamic overall heat transfer coefficient (W m^{-2} K^{-1});
h_0 - outer convective heat transfer coefficient (W m^{-2} K^{-1});
h_i - inner convective heat transfer coefficient (W m^{-2} K^{-1});
K_c - thermal conductivity (W m^{-1} K^{-1}); and,
L_c - covering material thickness (m).
h_0 and h_i can be estimated as shown in Eqs. 11 and 12.

$$h_0 = 2.8 + 1.2W_v \quad (11)$$

$$h_i = 1.52\left(T_{in} - T_{ex}\right)^{1/3} + 5.2\left(A_{GH} \times S_G \times L\right)^{1/2} \quad (12)$$

where:
W_v - wind velocity (m s^{-1});
S_G - section of the hydroponic greenhouse (m²); and,
L - length of the hydroponic greenhouse (m).

The heat transfer from the greenhouse floor Q_f and the amount of heat due to the perimeter Q_p are given in Eqs. 13 and 14.

$$Q_f = K_s \times d^{-1} \times A_f \left(T_{in} - T_s\right) \quad (13)$$

$$Q_p = F_p \times P_G \left(T_{in} - T_{ex}\right) \quad (14)$$

where:
K_s - thermal conductivity of the soil (W m^{-1} K^{-1});
d - depth of constant soil temperature (m);
T_s - desired water temperature (°C);
F_p - perimeter heat loss factor (W m^{-1} K^{-1}); and,
P_G - perimeter of the hydroponic greenhouse (m).

Heat loss by long wave radiation Q_{lw} is given by Eq. 15.

$$Q_{lw} = h_0 \times A_{GH} \times (1 - \tau) \times \left(T_{in} - T_{ex}\right) \quad (15)$$

Sky temperature T_{sky} is calculated as given by Eq. 16.

$$T_{sky} = 0.552 \times \left(T_{ex} + 273.15\right)^{3/2} - 273.15 \quad (16)$$

where:
T_{sky} - sky temperature (°C).

Heat loss by evaporation Q_{evap} is expressed as in Eq. 17.

$$Q_{evap} = M_T \times L_V \quad (17)$$

$$M_T = A_p \times p \times \left(W_{ps} - W_i\right) \times \left(R_a + R_s\right)^{-1} \quad (18)$$

where:
M_T - moisture transfer rate (kg s^{-1}); and,
L_V - latent heat of water vaporisation (J kg^{-1}).

The plant area A_p (m²) is calculated from the leaf area of the plant, then the saturated humidity ratio of air at the plant temperature, W_{ps} and the humidity ratio of air at the indoor temperature W_i can be calculated as follows in Eqs. 19 and 20.

$$W_{ps} = 0.6219P_{ws} \times \left(101.325 - P_{ws}\right)^{-1} \quad (19)$$

$$W_i = 0.6219P_w \times \left(101.325 - P_w\right)^{-1} \quad (20)$$

where:
P_{ws} - partial pressure at saturation (kPa); and,
P_w - partial pressure of the water vapour (kPa).

The expression of the real vapour pressure is shown in Eq. 21 (Khafajeh et al., 2023).

$$P_{ws} = e^{\left(C_1 \cdot 10^3 \cdot a^{-1} + C_2 - C_3 \cdot 10^{-3} \cdot a + C_4 \cdot 10^{-6} \cdot a^2 - C_5 \cdot 10^{-9} \cdot a^3 + C_6 \cdot \ln(a)\right)} \times 10^{-3} \quad (21)$$

Table 3 presents the values of the parameters of Eq. 21.

$$P_w = P_{ws} \times R_h \quad (22)$$

$$R_a = 220L_f^{0.2} \times V_i^{-0.8} \quad (23)$$

$$R_s = 200\left[1 + \left(e^{0.05(\tau \cdot I_{sr} - 50)}\right)^{-1}\right] \quad (24)$$

where:
R_h - relative air humidity (%);
R_a - aerodynamic resistance (s m^{-1}); and,
R_s - stomatal resistance (s m^{-1}).

The heat gain due to the release of CO_2 is expressed in Eq. 25 below.

$$Q_{co2} = \frac{0.278NHV \times MFR \times A_f}{PR} \quad (25)$$

where:
NHV- heating value of fuel (MJ kg^{-1});
MFR - CO_2 flow rate (kg m^{-2} per hour); and,
PR - Prandtl coefficient.

Table 3. Values of a, C1, C2, C3, C4, C5 and C6

Designation	Value
a	T_{in}+237.15
C1	-5.80002
C2	1.3915
C3	48.64024
C4	41.764768
C5	14.45209310
C6	6.5459673

a - Inner temperature (K); C1 to C6 - Constants

Results and Discussion

It is aimed to improve the energy model by incorporating the previously neglected loss parameters Q_{lw}, Q_f, Q_p, Q_{evap}, and Q_{water}, as well as the lighting heat gain Q_{co2} and Q_{sr}, without considering the effect of lighting. This will make it possible to

determine the most suitable shape and covering material for the hydroponic greenhouse.

Figure 5 below illustrates the heating and cooling requirements for the vinery shape with a polyvinyl chloride film cover throughout the year (Abd El-kader et al., 2013; Ghobadian et al., 2022; Khafajeh et al., 2023; Vincentdo et al., 2023). From the results presented in Table 4, it is evident that the vinery shape with a polyvinyl chloride film cover is the most energy-efficient option, as long as the covering material is properly installed. In contrast, older models would have considered the Quonset shape with the same covering material to be the least efficient in terms of energy and thus more costly.

Figure 6 displays the simulation of the IBGH model without lighting, which was created using Matlab software.

To determine the artificial light requirements for lettuce plants, the calculation involved hourly lighting energy requirements in watts to account for the heat produced

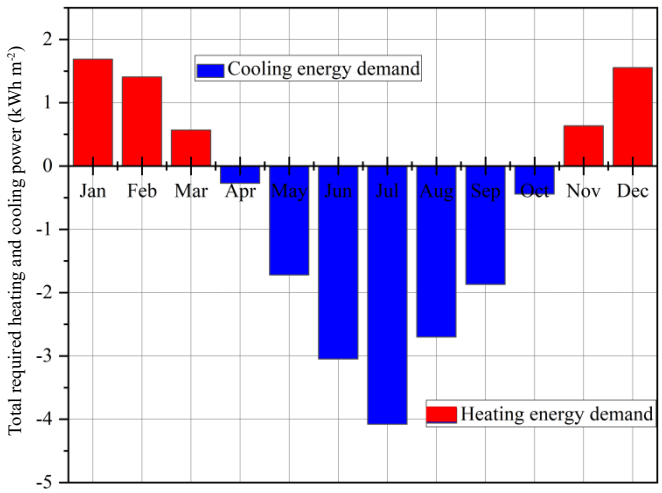

Figure 5. Estimation of the heating and cooling load of the vinery form

Table 4. The daily average heating and cooling demand of the model, excluding the impact of lighting (kWh m^{-2})

		Types of hydroponic greenhouses				
		Even span	Uneven span	Elliptic	Quonset	Vinery
Average cooling+ heating (kWh m^{-2})	M1	3.67386995	3.68021227	3.665550788	3.630700788	3.639194481
	M2	4.131694738	4.14123206	4.119184722	4.066778711	3.931693364
	M3	3.550146091	3.557858788	3.540029419	3.497649424	3.370546393
	M4	3.647210484	3.653497531	3.638963821	3.604417531	3.490976366
	M5	3.348730237	3.355090656	3.340387334	3.305437879	3.190740963
	M6	4.215829281	3.405298119	3.389584228	3.352232675	3.240829221

M1 - Glass covering; M2 - Low emissivity glass covering; M3 - Polyethylene film covering; M4 - Polycarbonate covering; M5 - Polyvinyl chloride covering; M6 - Ethylene-vinyl acetate copolymer EVA covering

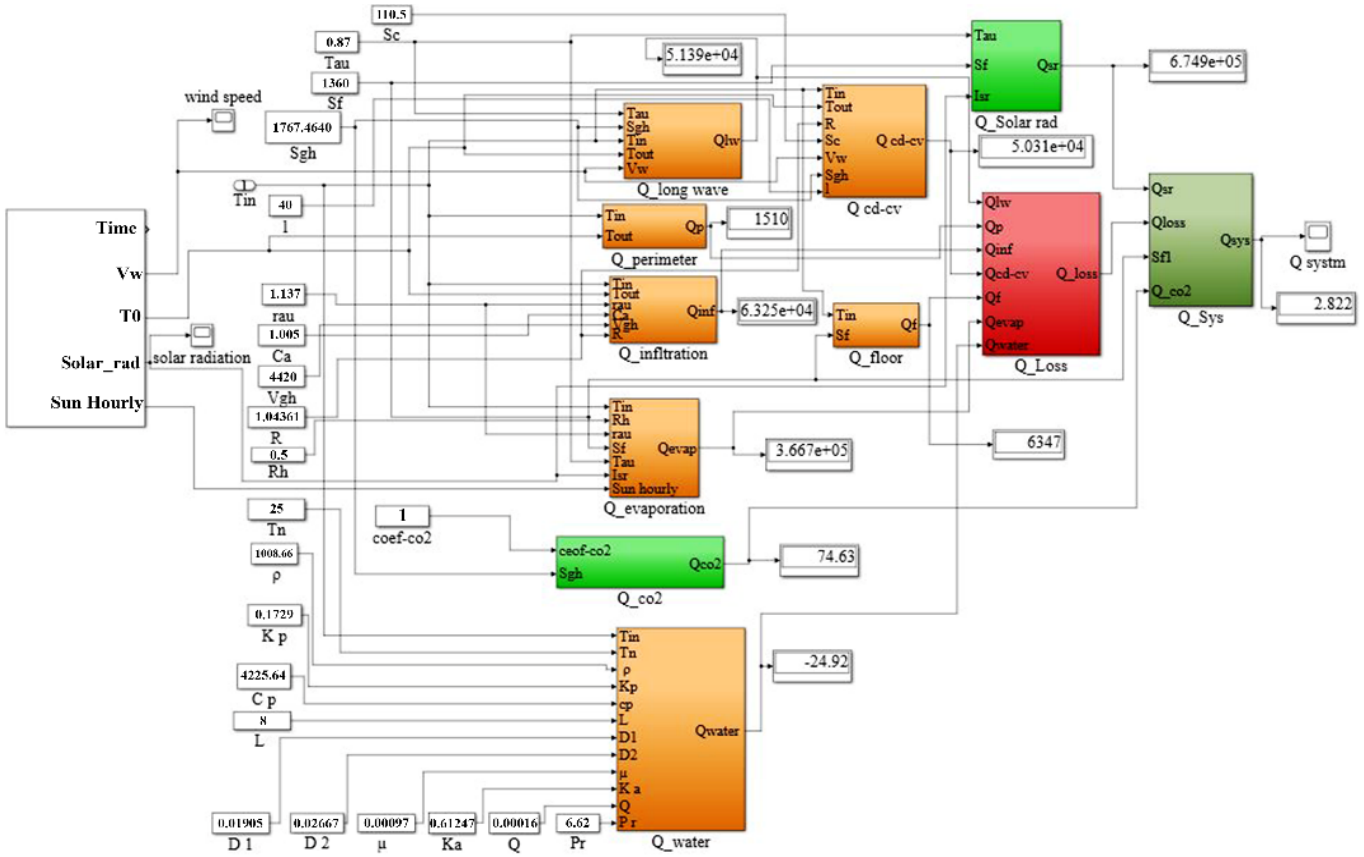

Sgh - Hydroponic greenhouse area (m²); T_{in} - Inner air temperature (°C); T_{out} - Average outdoor temperature (°C); V_w - Wind velocity (m s^{-1}); R - Number of air changes per hour (m^3 s^{-1}); rau - Density of internal air (kg m^{-3}); C_a - Specific heat of air (J kg^{-1} K^{-1}); V_{gh} - Volume of the hydroponic greenhouse (m^3); K_p - Thermal conductivity of pipe (W m^{-1} K^{-1}); A_1 - Inner area of pipe (m²); A_2 - Outer area of pipe (m²); D_2 - Outer diameter of pipe (m); D_1 - Inner diameter of pipe (m); L - Length of pipe (m); p - Density of the fluid (kg m^{-3}); u - Dynamic viscosity of the fluid (kg m^{-1} s^{-1}); Pr - Prandtl coefficient; Ka - Thermal conductivity of water (W m^{-1} K^{-1}); Cp - Specific heat (J kg^{-1} K^{-1}); T_n - Temperature of solution (°C); Q - Water flow (m^3 s^{-1}); A_f - Greenhouse floor area (m²); Tau - Transmissivity of the greenhouse cover; I_{sr} - Solar radiation on the horizontal surface (W m^{-2}); Sf - Floor surface (m²); Rh - Relative air humidity (%)

Figure 6. Block Simulink of the vinery form without lighting

by the lighting systems. Given a photoperiod of 16 hours, the lettuce plants' lighting requirement of 10.92 klux was determined, and then the daily light was calculated to ensure optimal growth conditions. The design of a natural lighting system begins with creating 3D models of hydroponic greenhouses covered with different materials (M1 to M6) to determine the necessary artificial lighting for the plants. To simulate daily light conditions, an appropriate sky type was chosen and the day and hours for a given moment in the year were specified. The simulation was run on the 1st, 8th, 15th, and 22nd day of each month, from 7:00 a.m. to 10:00 p.m., with a two-hour interval. Figure 7 shows the average illuminance received by different greenhouse shapes covered with M2 material throughout the year. It was deduced that the elliptic shape with M2 material is the least efficient in terms of daylight, while the uneven span shape is the best. To examine how different cladding materials affect daytime illumination, DIALUX EVO was used to simulate various cladding materials at a reference date and time (June 15, 2022, at 1:00 p.m.). Illumination is influenced by the greenhouse's height, size, and shape, as well as the cladding's transmission, reflection, and absorption of sunlight. The results are presented in the Table 5, providing insight into the relevant gain/illumination for different greenhouse types with specific construction materials and applied hydroponic greenhouse types (Du et al., 2012; Kittler et al., 2014).

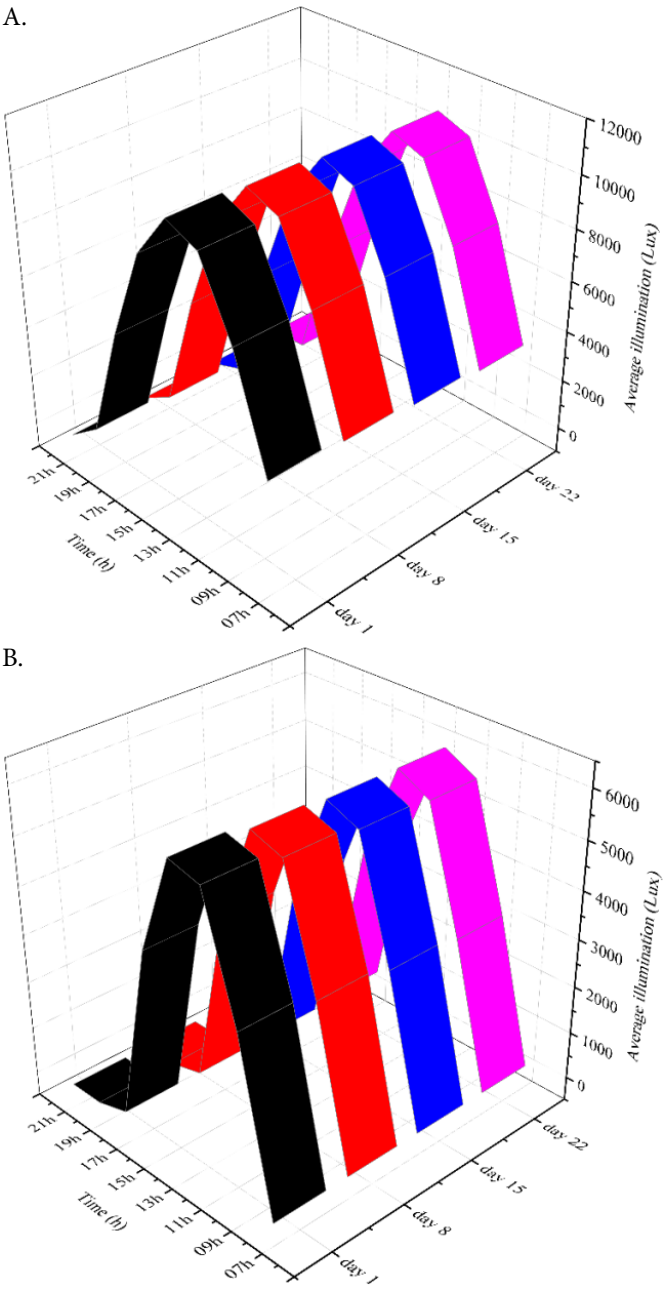

Figure 7. The outcomes of the daylight simulation during August (A) and December (B)

Table 5 presents the daylight values for each hydroponic greenhouse shape. It is observed that M3 and M5 have lower light values, while the uneven span hydroponic greenhouse has the highest lux level value. The remaining shapes are almost identical in terms of lighting. The process of designing the daylighting system begins with creating a 3D model of the covered hydroponic greenhouse using M1 to M6 materials. To achieve the desired 10.92 klux level of illumination for the lettuce plants, the following steps were followed to determine the necessary artificial lighting requirements. Figure 8 presents the natural lighting conditions examined for all the analyzed hydroponic greenhouse types.

Figure 9 displays the annual average daylight levels for various hydroponic greenhouse types.

To meet the target lux level of 10.92 klux for the lettuce plants (Ma et al., 2019; Liu et al., 2020; Ravankar et al., 2020), the process outlined in Figure 10 was used to design the necessary artificial lighting.

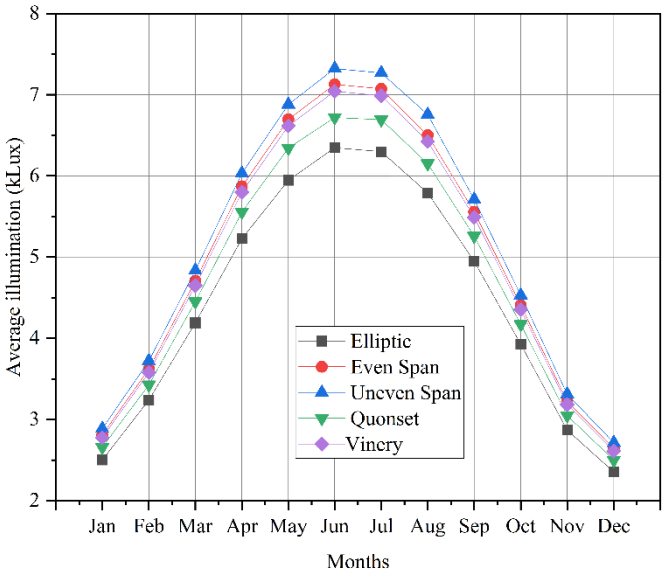

Figure 8. Natural lighting for all types of hydroponic greenhouses analyzed

Table 5. Influence of the materials used for the covering of structure

Covering materials	Loss/gain of natural light (%)	Lighting simulated at June 15, 2022, 13 hours
M1	-3.37	10757
M2	0.00	11176
M3	-13.44	9636
M4	1.58	11308
M5	-6.73	10383
M6	1.58	11308

M1 - Glass covering; M2 - Low emissivity glass covering; M3 - Polyethylene film covering; M4 - Polycarbonate covering; M5 - Polyvinyl chloride covering; M6 - Ethylene-vinyl acetate copolymer EVA covering

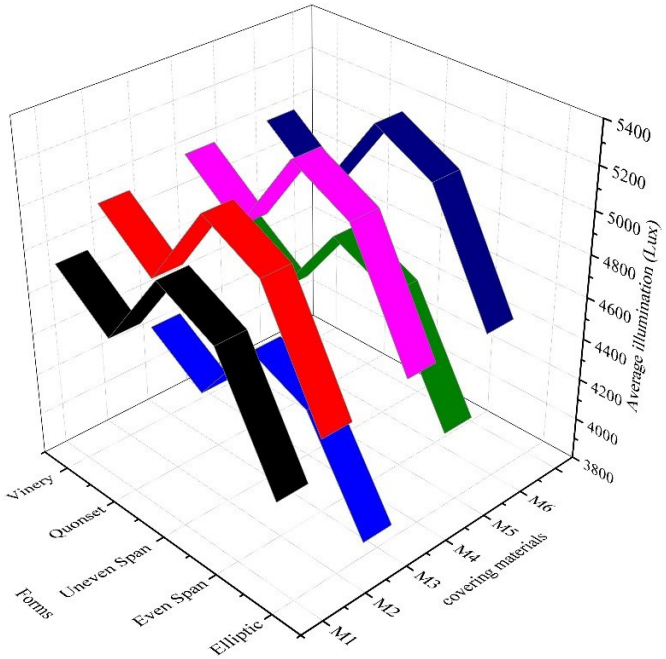

M1 - Glass covering; M2 - Low emissivity glass covering; M3 - Polyethylene film covering; M4 - Polycarbonate covering; M5 - Polyvinyl chloride covering; M6 - Ethylene-vinyl acetate copolymer EVA covering

Figure 9. The average daylight level throughout the year for all types of hydroponic greenhouses

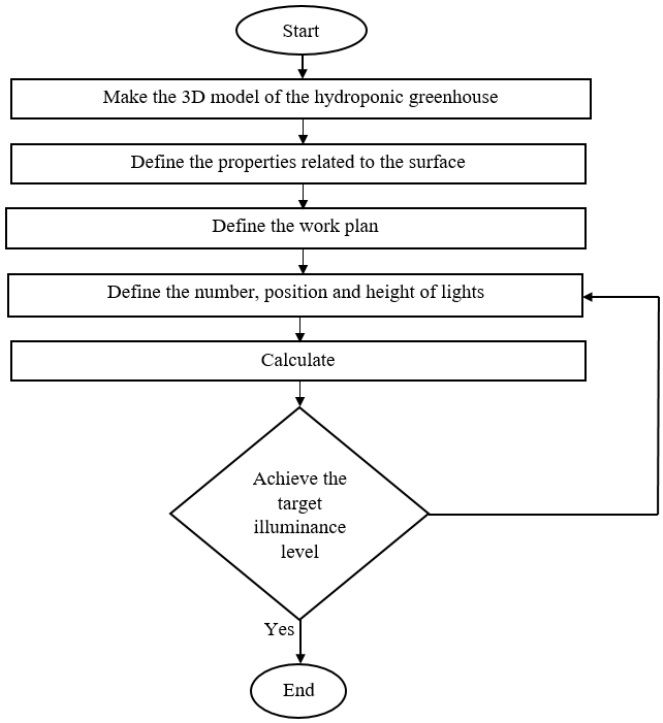

Figure 10. Lighting design process

To achieve the desired lighting level of 10.92 klux, compared to the target level of 10.99 klux, the simulation results indicate that 3699 luminaires must be used, each with a power of 60 W, suspended at a height of 1.8 m. Additionally, the luminous efficacy of each luminaire should be 160 lm W^{-1}, with a changing colour temperature CCT of 4000 K and a consumption rate of 163 W m^{-2}. Based on the false colour rendering, the lighting distribution is uniform in all parts of the space, and the illuminance level is approximately at the desired level.

An intelligent light sensor is connected to a controller, which acquires real-time values of natural light emitted in the greenhouse to reduce light energy consumption. After all the calculations, a difference was found between the desired and actual values, which allows the regulation of the light level in the greenhouse uniformly, corresponding to the targeted value every hour from 7:00 a.m. to 10:00 p.m. When the daily PPFD is obtained, the lighting system is triggered automatically. To determine the average compensated illumination of the hydroponic greenhouse, the value of the implemented lights' illumination (when all the lights are on) is subtracted from the given daylight. To achieve low energy consumption throughout the year, it is essential to determine the compensated lighting demand in the hydroponic greenhouse, as shown in Figure 11 (Wang et al., 2019; Zhang et al., 2020; Karlowsky et al., 2021).

According to the calculation results in Figure 12, it is observed that the uneven span hydroponic greenhouse form has the least need for artificial lighting. The investigation will focus on determining whether the heat from the luminaires has a direct effect on the greenhouse's energy balance, despite the positive results so far regarding the choice of shape and coverage and their impact on the lighting system's efficiency. This energy amount made it possible to evaluate the light's misfortune from the lighting instrumentation in terms of energy, and the amount is calculated as follows (Eq. 26).

$$Q_{li} = K' \times K'' \times W_l \quad (26)$$

where:

W_l - lighting energy consumption (W);

K'- lighting allowance factor; and,

K" - heat conversion factor.

Figure 12 presents the annual demand for lighting energy.

As a result of the calculations, Figures 13 and 14 show the annual heat gains and losses in the hydroponic greenhouse. The total heat gain of the greenhouse is the sum of the heat gain due to solar radiation, the lighting system, and the CO_2

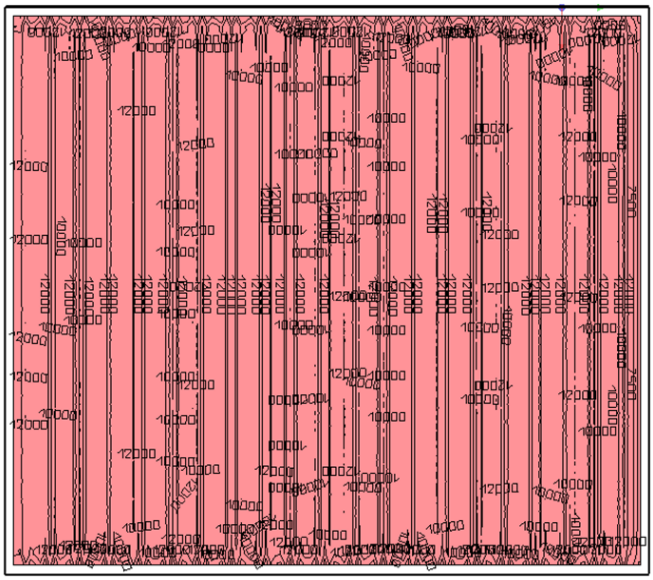

Figure 11. False colour rendering of the light distribution on the hydroponic greenhouse plan

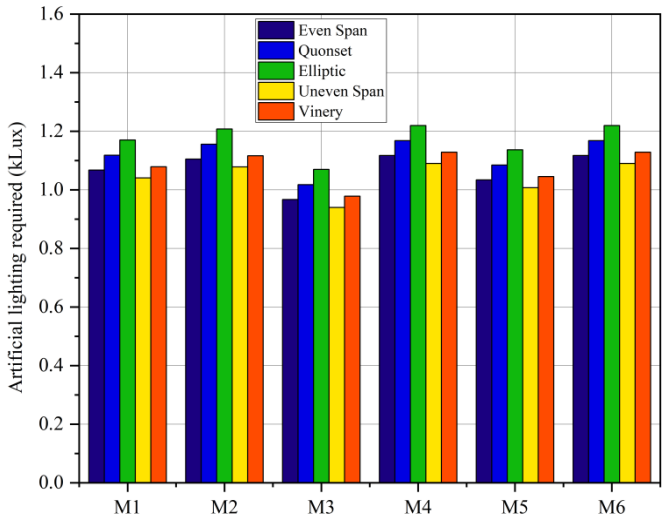

M1 - Glass covering; M2 - Low emissivity glass covering; M3 - Polyethylene film covering; M4 - Polycarbonate covering; M5 - Polyvinyl chloride covering; M6 - Ethylene-vinyl acetate copolymer EVA covering

Figure 12. Annual lighting energy demand

concentrator, and all these results are shown in Figure 13. It is observed that the total heat gain curve closely follows the heat gain curve due to solar radiation throughout the year, except for the summer months. This is expected, as the demand for artificial lighting during June, July, and August is very low due to the abundance of daylight.

Figure 14 illustrates all the heat losses present in the hydroponic system, including Q_{cd-cv}, Q_{inf}, Q_{evap}, Q_{lw}, Q_{floor}, Q_p, Q_{li} and Q_{water}. A prototype of the hydroponic greenhouse system under investigation was developed in order to test the accuracy of the heat balance system. The structure of this system took the same form as the traditional system, which is the even span (width: 34 m, length: 40 m, height: 4.35 m) enclosed by a 3.2 mm-thick glass material. Figure 15 illustrates the proposed prototype, which was integrated with a Raspberry Pi3, along with two DHT11 sensors for monitoring both internal and external levels of humidity and temperature. Additionally, the necessary actuators were installed and connected, including a heater, fan, humidifier, dehumidifier, CO_2 and lighting to effectively regulate the internal environment's humidity and temperature.

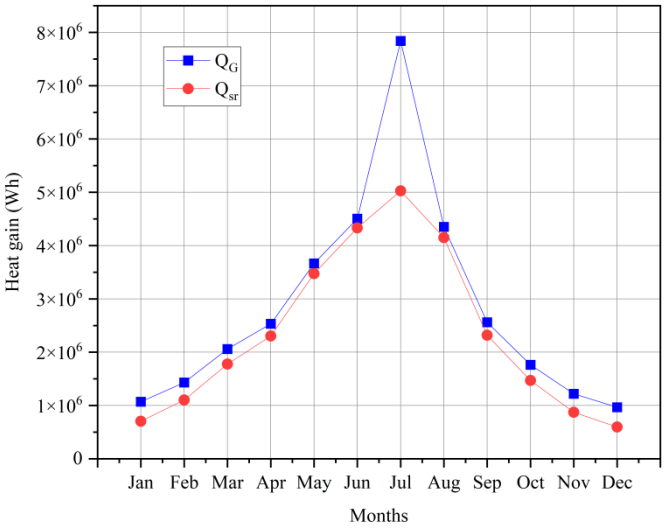

Q_G - Total heat gain inside the greenhouse (W); Q_{sr} - Solar radiation heat gain (W)

Figure 13. Monthly evolution of heat gain

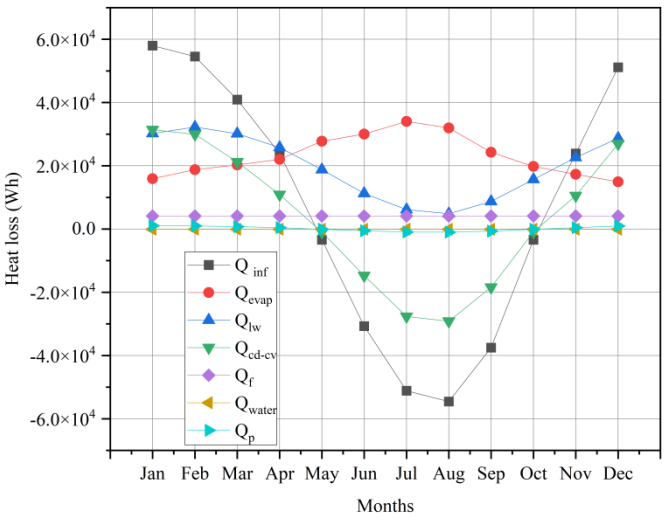

Q_{inf} - Infiltration heat transfer (W); Q_{evap} - Evapotranspiration heat transfer (W); Q_{lw} - Long-wave radiation heat transfer (W); Q_{cd-cv} - Conduction and convection heat transfer (W); Q_f - Floor heat transfer (W); Q_{water} - Water heat transfer (W); Q_p - Perimeter heat transfer (W)

Figure 14. Monthly evolution of heat loss

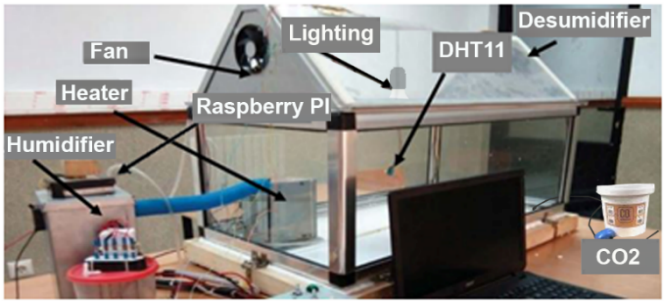

Fan - Actuator of cooling; Heater - Actuator of heating; Humidifier - Actuator of humidification; Dehumidifier - Actuator of dehumidification; DHT11 - Temperature and humidity sensor; Lighting - Actuator of lighting; CO_2 - CO_2 generator; Raspberry Pi - Controller

Figure 15. Prototype of the hydroponic system

Then the measurement of the internal temperature T_{in} was carried out to verify the accuracy of the designed system compared to the simulated model under the MATLAB Simulink Platform.

Figure 16 provides a visual representation of the disparity between the measured internal climate parameters and their simulated counterparts. This graphical representation serves as a crucial tool for evaluating the performance of the designed heat balance system in replicating real-world conditions.

The close alignment between the measured and simulated climate parameters depicted in Figure 16 is a compelling indication of the precision achieved by the designed system, the error of which does not exceed 6%. The minimal discrepancy observed signifies that the model accurately replicates the complex interplay of various climatic factors. The figure's data reaffirms confidence in the reliability and effectiveness of the designed system in faithfully emulating real-world climate conditions.

Following the validation of the model against the measured data, the subsequent step involves a comparative analysis. Initially, the assessment will cover models of various hydroponic systems (including the traditional model and those including the new injected heat loss and gain parameter, without lighting effects and with lighting enhancements), all of which feature an even span configuration and are equipped

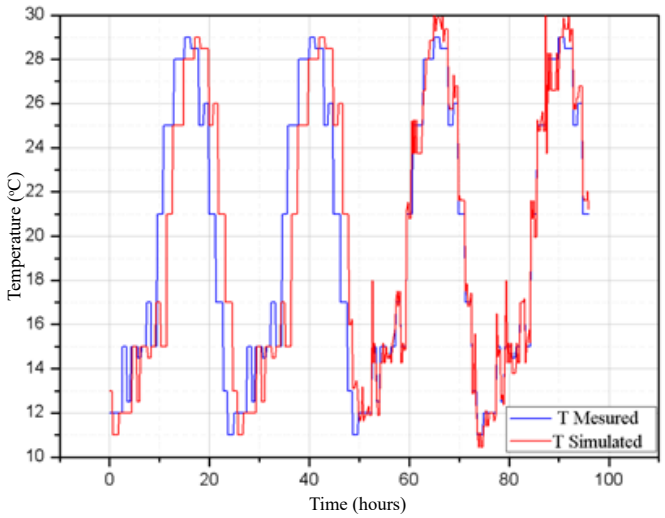

T Measured - Measured inner temperature; T simulated - Simulated inner temperature

Figure 16. Evolution of the simulated and the measured internal temperature

with M1 glass coverings. This comparative evaluation will provide valuable insights into the performance disparities across these different systems, shedding light on the efficacy of the proposed enhancements.

To enhance the assessment of the energy balance across the various models, a comparison has been made with the total energy consumption measured within the hydroponic greenhouse, as depicted in Figure 17.

In Figure 17, it is clear that the system demonstrates a high level of accuracy, with an error rate consistently below 6%, even when the impact of lighting effects is taken into account. Notably, when focusing solely on parameters related to heat gain and heat loss, without taking into account the effects of lighting, the accuracy of the system decreases significantly, with an error rate in excess of 11%. Furthermore, compared with traditional models, the system becomes less accurate, with an error rate well over 36%, underlining the superior performance and efficiency of this approach.

In the subsequent phase of the analysis, a comprehensive comparison will be conducted between the conventional hydroponic model and the meticulously designed system, which incorporates the neglected parameter and the optimization of the hydroponic system shape and its covering material. Figure 18 shows the energy demand of the different studied models.

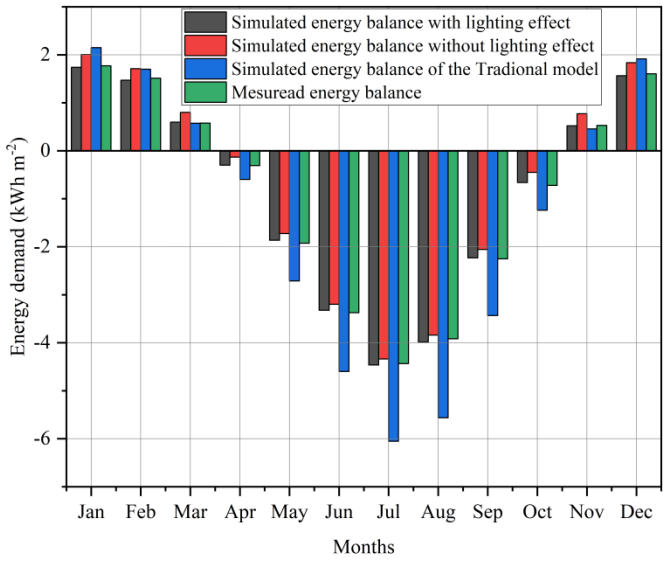

Figure 17. Monthly evolution of the simulated and the measured of energy demand

Based on the results presented above, it is evident that the traditional model's estimate of energy demand is not reliable. However, the model has been improved by taking into account the previously ignored factors. To provide better and more accurate results, the IBGH model was created, which proves the significant effect of lighting heat on the energy demand for heating and cooling in a hydroponic system. The energy demand for lighting, cooling, and heating equipment for the different forms of hydroponic greenhouses studied as a function of the covering films is illustrated in Table 6.

The presented results demonstrate the significance of the lighting equipment and other previously overlooked parameters on the overall energy demand in a hydroponic system. The established model has effectively captured these important factors, which have been shown to have a substantial impact on the energy requirements of the system.

In the future, research should focus on integrating advanced sensors and automation for precise environmental control. Exploring innovative covering materials like nanocomposites and smart films holds promise for improving light transmission and durability. Additionally, integrating renewable energy sources and employing advanced modelling techniques can further enhance greenhouse efficiency.

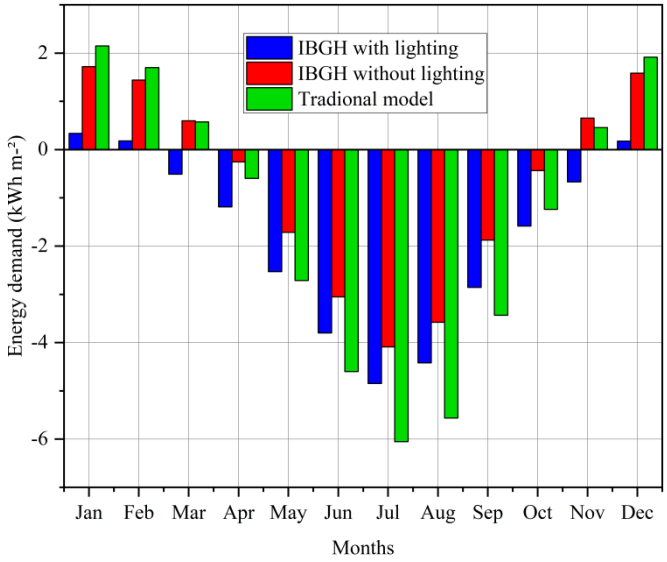

IBGH with lighting - Developed greenhouse within the direct and indirect effect of lighting; IBGH without lighting -Developed greenhouse without the direct and indirect effect of lighting; Traditional model - Literature greenhouse model

Figure 18. Monthly evolution of energy demand

Table 6. Total energy demand (kWh m^{-2})

	Even span	Uneven span	Elliptic	Quonset	Vinery
M1	3.6	3.7	3.0	3.5	3.8
M2	3.9	4.1	3.4	3.8	4.1
M3	3.4	3.6	2.8	3.3	3.5
M4	3.6	3.7	3.0	3.5	3.7
M5	3.3	3.4	2.7	3.2	3.4
M6	3.3	3.4	2.8	3.2	3.4

M1 - Glass covering; M2 - Low emissivity glass covering; M3 - Polyethylene film covering; M4 - Polycarbonate covering; M5 - Polyvinyl chloride covering; M6 - Ethylene-vinyl acetate copolymer EVA covering

Conclusions

1. The study emphasises the importance of a meticulous approach in selecting roofing materials and greenhouse design to minimise energy consumption. Through the identification of optimal configurations and consideration of previously overlooked parameters, the groundwork has been laid for enhancing efficiency and sustainability in hydroponic greenhouse systems. The findings suggest that an elliptical structure and PVC as a covering material offer practical advantages.

2. The findings from the preceding studies underscore the substantial influence of lighting equipment and previously overlooked parameters on the overall energy demand in hydroponic systems. The introduction of the novel Integrated Hydroponic Greenhouse Model (IBGH) provides a crucial revelation, emphasizing that the consideration of lighting heat plays a pivotal role in achieving energy-efficient heating and cooling processes. This insight not only advances the understanding of the energy dynamics in hydroponics but also paves the way for the adoption of greener and more resource-efficient practices in the field.

3. The IBGH model, by addressing the intricate relationship between lighting and thermal management, represents a significant stride towards optimizing sustainability in hydroponic cultivation.

Literature Cited

Abd El-kader, S. M.; Mohammad El-Basioni, B. M. Precision farming solution in Egypt using the wireless sensor network technology. Egyptian Informatics Journal, v.14, p.221-233, 2013. https://doi.org/10.1016/j.eij.2013.06.004

Akram, M.; Riaz, M.; Noreen, S.; Shariati, M. A.; Shaheen, G.; Akhter, N.; Parveen, F.; Akhtar, N.; Zafar, S.; Owais Ghauri, A.; Riaz, Z.; Khan, F. S.; Kausar, S.; Zainab, R. Therapeutic potential of medicinal plants for the management of scabies. Dermatologic Therapy, v.33, p.1-7, 2020. https://doi.org/10.1111/dth.13186

Al-Karaki, J. N.; Ul-Mustafa, R.; Kamal, A. E. Data aggregation and routing in Wireless Sensor Networks: Optimal and heuristic algorithms. Computer Networks, v.53, p.945-960, 2009. https://doi.org/10.1016/j.comnet.2008.12.001

Aryai, V.; Goldsworthy, M. Controlling electricity storage to balance electricity costs and greenhouse gas emissions in buildings. Energy Informatics, v.5, p.1, 2022. https://doi.org/10.1186/s42162-022-00216-5

Belkadi, A.; Mezghani, D.; Mami, A. Design and implementation of FLC applied to a smart greenhouse. Engenharia Agrícola, v.40, p.777-790, 2020. https://doi.org/10.1590/1809-4430-eng.agric.v40n6p777-790/2020

Belkadi, A.; Mezghani, D.; Mami, A. Energy design and optimization of a greenhouse: a heating, cooling and lighting study. Engineering, Technology & Applied Science Research, v.9, p.4235-4242, 2019. https://doi.org/10.48084/etasr.2787

Belkadi, A.; Mezghani, D.; Mami, A. Energy study of a greenhouse and optimisation of the choice of shape and covering material: Based on an improved static model. Engenharia Agrícola, v.4, p.297-310, 2021. https://doi.org/10.1590/1809-4430-Eng.Agric.v41n3p297-310/2021

Bouadila, S.; Baddadi, S.; Ben Ali, R.; Ayed, R.; Skouri, S. Deploying low-carbon energy technologies in soilless vertical agricultural greenhouses in Tunisia. Thermal Science and Engineering Progress, v.42, p.101896, 2023. https://doi.org/10.1016/j.tsep.2023.101896

Cannarsa, P.; Lucarini, V.; Martinez, P.; Urbani, C.; Vancostenoble, J. Analysis of a two-layer energy balance model: Long time behavior and greenhouse effect. Chaos: An Interdisciplinary Journal of Nonlinear Science, v.33, p.11, 2023. https://doi.org/10.1063/5.0136673

Delgado, A. E.; Chaparro, W. A.; Cáceres, R. G. Effect of modified greenhouse covers on the development of plants of *Lycopersicon esculentum mill*. Dyna, v.87, p.91-97, 2020. https://doi.org/10.15446/dyna.v87n213.81082

Du, J.; Bansal, P.; Huang, B. Simulation model of a greenhouse with a heat-pipe heating system. Applied Energy, v.93, p.268-276, 2012. https://doi.org/10.1016/j.apenergy.2011.12.069

Ezzaeri, K.; Fatnassi, H.; Bouharroud, R.; Gourdo, L.; Bazgaou, A.; Wifaya, A.; Demrati, H.; Bekkaoui, A.; Aharoune, A.; Poncet, C.; Bouirden, L. The effect of photovoltaic panels on the microclimate and on the tomato production under photovoltaic canarian greenhouses. Solar Energy, v.173, p.1126-1134, 2018. https://doi.org/10.1016/j.solener.2018.08.043

Ghobadian, F.; Moghaddasi, R.; Kazemnejad, M. DEA-based efficiency assessment of greenhouse red-leaf lettuce production in Iran using vertical hydroponic method. Agricultural Research, v.12, p.197-207, 2022. https://doi.org/10.1007/s40003-022-00635-6

Gillani, S. A.; Abbasi, R.; Martinez, P.; Ahmad, R. Review on energy efficient artificial illumination in aquaponics. Cleaner and Circular Bioeconomy, v.2, p.100015, 2022. https://doi.org/10.1016/j.clcb.2022.100015

Karlowsky, S.; Gläser, M.; Henschel, K.; Schwarz, D. Seasonal nitrous oxide emissions from hydroponic tomato and cucumber cultivation in a commercial greenhouse company. Frontiers in Sustainable Food Systems, v.5, p.1-13, 2021. https://doi.org/10.3389/fsufs.2021.626053

Khafajeh, H.; Banakar, A.; Minaei, S.; Delavar, M. A hydroponic greenhouse fuzzy control system: design, development and optimization using the genetic algorithm. Spanish Journal of Agricultural Research, v.21, p.1-12, 2023. https://doi.org/10.5424/Sjar/2023211-19392

Kittler, R.; Darula, S. The simultaneous occurrence and relationship of sunlight and skylight under ISO/CIE standard sky types. Lighting Research & Technology, v.47, p.565-580, 2014. https://doi.org/10.1177/1477153514538883

Kumar, S. A.; Ilango, P. The impact of wireless sensor network in the field of precision agriculture: A review. Wireless Personal Communications, v.98, p.685-698, 2017. https://doi.org/10.1007/s11277-017-4890-z2

Liu, G.; Nouaze, J. C.; Touko Mbouembe, P. L.; Kim, J. H. YOLO-Tomato: A robust algorithm for tomato detection based on YOLOv3. Sensors, v.20, p.2145, 2020. https://doi.org/10.3390/s20072145

Luna-Fletes, J. A.; Cruz-Crespo, E.; Can-Chulim, Á. Piedra pómez, tezontle y soluciones nutritivas en el cultivo de tomate cherry. Revista Terra Latinoamericana, v.39, p.1-12, 2021. https://doi.org/10.28940/terra.v39i0.781

Ma, D.; Carpenter, N.; Maki, H.; Rehman, T. U.; Tuinstra, M. R.; Jin, J. Greenhouse environment modeling and simulation for microclimate control. Computers and Electronics in Agriculture, v.162, p.134-142, 2019. https://doi.org/10.1016/j.compag.2019.04.013

Pawlowski, A.; Beschi, M.; Guzmán, J. L.; Visioli, A.; Berenguel, M.; Dormido, S. Application of SSOD-PI and PI-SSOD event-based controllers to greenhouse climatic control. ISA Transactions, v.65, p.525-536, 2016. https://doi.org/10.1016/j.isatra.2016.08.008

Ravankar, A.; Ankit, R. A.; Watanabe, M.; Hoshino, Y.; Rawankar, A. Development of a low-cost semantic monitoring system for vineyards using autonomous robots. Agriculture, v.10, p.1-19, 2020. https://doi.org/10.3390/agriculture10050182

Vincentdo, V.; Surantha, N. Nutrient film technique-based hydroponic monitoring and controlling system using ANFIS. Electronics, v.12, p.1446, 2023. https://doi.org/10.3390/electronics12061446

Wang, Y. S.; Shen, C. Y.; Jiang, J. G. Antidepressant active ingredients from herbs and nutraceuticals used in TCM: Pharmacological mechanisms and prospects for drug discovery. Pharmacological Research, v.150, p.104520, 2019. https://doi.org/10.1016/j.phrs.2019.104520

Zaborowska, E.; Czerwionka, K.; Mąkinia, J. Integrated plant-wide modelling for evaluation of the energy balance and greenhouse gas footprint in large wastewater treatment plants. Applied Energy, v.282, p.116126, 2021. https://doi.org/10.1016/j.apenergy.2020.116126

Zhang, Y.; Long, Y.; Yu, S.; Li, D.; Yang, M.; Guan, Y.; Zhang, D.; Wan, J.; Liu, S.; Shi, A.; Li, N.; Peng, W. Natural volatile oils derived from herbal medicines: A promising therapy way for treating depressive disorder. Pharmacological Research, v.164, p.105376, 2020. https://doi.org/10.1016/j.phrs.2020.105376